

# Chapter 12

## The WHISPER Relaxation Sounder and the CLUSTER Active Archive

J.G. Trotignon, P.M.E. Décréau, J.L. Rauch, X. Vallières, A. Rochel, S. Kouglbléno, G. Lointier, G. Facskó, P. Canu, F. Darrouzet, and A. Masson

**Abstract** The Waves of High frequency and Sounder for Probing of Electron density by Relaxation (WHISPER) instrument is part of the Wave Experiment Consortium (WEC) of the CLUSTER mission. With the help of the long double sphere antennae of the Electric Field and Wave (EFW) instrument and the Digital Wave Processor (DWP), it delivers active (sounding) and natural (transmitter off) electric field spectra, respectively from 4 to 82 kHz, and from 2 to 80 kHz. These frequency ranges have been chosen to include the electron plasma frequency, which is closely related to the total electron density, in most of the regions encountered by the CLUSTER spacecraft. Presented here is an overview of the WHISPER data products available in the CLUSTER Active Archive (CAA). The instrument and its performance are first recalled. The way the WHISPER products are obtained is then described, with particular attention being paid to the density determination. Both sounding and natural measurements are commonly used in this process, which depends on the ambient plasma regime. This is illustrated using drawings similar to the Bryant plots commonly used in the CLUSTER master science plan. These give a clear overview of typical density values and the parts of the orbits where they are obtained. More information on the applied software or on the quality/reliability of the density determination can also be highlighted.

---

J.G. Trotignon (✉), P.M.E. Décréau, J.L. Rauch, X. Vallières, A. Rochel, S. Kouglbléno, G. Lointier, and G. Facskó  
Laboratoire de Physique et Chimie de l'Environnement et de l'Espace, Université d'Orléans, Orléans, France  
e-mail: Jean-Gabriel.Trotignon@cnrs-orleans.fr; pdecreau@cnrs-orleans.fr;  
jlrauch@cnrs-orleans.fr; Xavier.Vallieres@cnrs-orleans.fr; alban.rochel@gmail.com;  
sena.kouglbléno@cnrs-orleans.fr; guillaume.lointier@cnrs-orleans.fr;  
Gabor.Facsko@cnrs-orleans.fr

P. Canu  
Laboratoire de Physique des Plasmas, Vélizy, France  
e-mail: patrick.canu@lpp.polytechnique.fr

F. Darrouzet  
Institut d'Aéronomie Spatiale de Belgique, Bruxelles, Belgique  
e-mail: Fabien.Darrouzet@ama.be

A. Masson  
RSSD, ESA, Noordwijk, The Netherlands  
e-mail: Arnaud.Masson@esa.int

## 12.1 Introduction

The CLUSTER Active Archive (CAA) has been created to house data delivered from all of the CLUSTER instruments and to make these data available to the wide scientific community [18]. In this context, the WHISPER (Waves of HIgh frequency and Sounder for Probing of Electron density by Relaxation) team provides two principal types of data: the total electron density at standard time resolutions of either 2.15 or 52 s, and electric field spectra in the frequency range 2–82 with time resolution 1.7 or 3.4 s. The total wave energy in the range 2–80 kHz is also provided with higher time resolutions. The density can be deduced from the characteristics of natural waves monitored whenever WHISPER is in natural mode (transmitter off) and/or from resonances triggered in the sounding mode. After a brief description of the instrument design and operation (Section 12.2) the data products ingested into CAA (Section 12.3) and some of the cross calibration activities (Section 12.5) are presented. The way the electron density is determined is then recalled (Section 12.4) with, as far as possible, a particular attention paid to the reliability, accuracy and degree of confidence (Sections 12.4 and 12.6).

## 12.2 WHISPER Instrument Design and Performance

The WHISPER experiment results from a collaboration between experimenters organised within the context of the Wave Experiment Consortium, WEC, which includes five instruments ([15, 26] *esp.* Sects. 1 and 4). The WHISPER instrument [6, 7] consists basically of a receiver, a transmitter, and a wave spectrum analyser, associated with parts of two other WEC instruments: the sensors of the Electric Field and Wave, EFW, experiment and data processing functions of the Digital Wave Processing, DWP, experiment. WHISPER is devoted to the survey, active and natural, of the WEC electric signal in the frequency range from about 2–82 kHz, which includes electrostatic and electromagnetic natural emissions of interest to the CLUSTER objectives, in particular in the vicinity of the plasma frequency from which the total electron density may be determined. Let us note that one of the main functions of the WHISPER experiment is to provide reference values of this fundamental plasma parameter.

Two modes of operation are used alternatively. The natural wave mode, when the transmitter stays on stand-by, and the sounding mode during which the transmitter triggers plasma resonances prior to reception. In both cases, a pair of EFW sensors is used as a double-sphere electric dipole antenna, whose potential difference is band-pass filtered, digitised, multiplied by a windowing function (to make the signal periodic), and finally analysed in frequency by an onboard FFT processor which computes a full frequency spectrum every 13.33 ms (40 ms/3) in normal telemetry operation (normal mode, NM), and in most burst mode (BM) usually every 26.6 or 40 ms (two or three times the basic WHISPER recurrence period of 13.33 ms). The spectrum covers the 0–83 kHz band in 512 bins or 256 bins, with a frequency

resolution of 162.8 Hz ( $F_{ech}/1024$  with the sampling frequency  $F_{ech} = 1$  MHz/6) in the 512-bin FFT option or 325.5 Hz in the 256-bin FFT option. The modulus of the complex amplitude in each bin is calculated, while the associated phase information is discarded. These spectral amplitude (moduli) are used for all subsequent onboard calculations. This choice of amplitude (rather than power) may appear curious, but there was a strong technical constraint: the dynamic range of the spectral power exceeds the dynamic range (limited by the word length) of the processors used by WHISPER, and also by DWP which, in some modes of operation, performs processing for WHISPER. The difference in the results obtained by summing the squares and summing the amplitudes is not large (less than 2 dB) for a wide-sense-stationary random process. A few bins are not transmitted to the CLUSTER telemetry (due to limited TM resource and input signal filtering), which explains why the 0–83 kHz band is not fully covered in the WHISPER data (as the WHISPER spectrum data size is always 512 in CAA, the missing bins are set to the -1.0 fill value).

In natural wave mode, successive spectra are accumulated onboard over intervals of 0.213 s (16 times 13.33 ms) to 0.853 s (64 times 13.33 ms) when in NM mode and of 0.107 s (8 times 13.33 ms) to 0.213 s (16 times 13.33 ms) when in BM mode, thus smoothing sporadic features and improving the signal to noise ratio. Moduli of the same frequency are thus summed onboard while averages are computed on ground. Each accumulated modulus is compressed quasi-logarithmically to a 6-bit word (or 8-bit word). At regular time intervals, one of these accumulated spectra is selected and transmitted to ground: between one out of ten and one out of two in NM mode, resulting in a time resolution in the range 1.7–3.4 s; and one out of three in BM mode, resulting in a time resolution of 0.320 or 0.640 s.

In all natural telemetry modes, the measured integrated power in the band 2–80 kHz, prior to windowing and FFT processings, is accumulated over each time acquisition, forming a quantity called “Energy”, available every 13.33 ms. In one option, available in BM telemetry, time series of “Energy” are transmitted to ground at full time resolution (13.33 ms), after a quasi-logarithmic compression of the “Energy” values to 8 bits (3 bits for the mantissa and 5 bits for the exponent; mantissa and exponent are described in Section 12.3.1). Otherwise, these “Energy” values are accumulated aboard over the same time interval as for the onboard accumulated-spectra. These values, also quasi-logarithmically compressed to 8 bits, are transmitted to the ground without further selection, i.e. with a time resolution better than that of the transmitted-to-ground accumulated spectra, by a factor between two and ten in NM telemetry mode and up to 48 in BM.

In sounding mode, a signal acquisition is performed a few milliseconds (4.9 or 5.2 ms) after transmission of a sounding pulse, the listening duration is at least 6.14 ms, which is compatible with a sampling frequency of 166.66 kHz and a 512-bin FFT. The sounding pulse is a short sinusoidal wave train whose frequency sweeps the 4–82 kHz band, or less depending on the operating mode, in steps of 976.6 Hz (1 MHz/1024) when the wave train duration is 1.024 ms and of 1953.1 Hz when the wave train duration is 0.512 ms. The spectral width of the emitted pulse is the inverse of its duration, and consequently the pulse can trigger all the characteristic frequencies of the medium within a band of 1 or 2 kHz around the pulse

frequency. The high spectral resolution of the FFT receiver allows the triggered frequencies to be identified as resonances, i.e. as very intense echoes which are strongly monochromatic and correspond to frequencies for which the group velocity is very small and close to the spacecraft velocity [3, 10].

In natural wave mode, the measured antenna potential difference is processed by FFT to compute a full frequency spectrum every 13.33 ms, while in sounding mode this computation is performed after every emission of a sounding pulse, at intervals equal to the step duration, 26.6 or 40 ms in most cases (two or three times the basic WHISPER recurrence period of 13.33 ms). As the telemetry resource does not allow all the onboard computed spectra to be downloaded the following compression strategy has been applied. It consists in selecting, in each full (0–83 kHz) spectrum associated to each sounding wave train, only the bins whose frequency is inside the frequency band ( $\sim 1$  or 2 kHz) of the emitted pulse. Those selected frequency bins contribute to a global “active/sounding” spectrum, obtained once the 4–82 kHz frequency sweep has been completed, which is downloaded. Let us note that 80 frequency steps of 976.6 Hz frequency bandwidth are for instance necessary to cover the full WHISPER frequency range. This corresponds to sweep duration of 3.2 s ( $80 \times 40$  ms) in the simplest mode, available as a back up operation option fully managed by the WHISPER electronic module. This back up option has been used on C4 CLUSTER satellite since September 2003, when part of the onboard WHISPER memory failed, probably due to severe environmental conditions. In other operational modes, DWP performs much of the WHISPER data processing. The most frequently used option has the emitter stepping by 976.6 Hz (pulse duration 1.024 ms) in the lower part of the frequency range, and by 1,953.1 Hz (pulses of 0.512 ms) at higher frequencies. With a step duration of 26.6 ms at all frequencies, the overall sweep duration is less than 1.5 s, which permits two sweeps within 3 s of a total sounding time interval. Other modes are available, with sweep duration between 0.5 and 10 s. Active spectrum values (moduli) are compressed quasi-logarithmically to 8-bit words before being transmitted to ground.

In addition to the frequency bins retained in each frequency step to construct a sounding spectrum (usually 6 bins, 162.8 Hz in bandwidth), bins whose frequency is far away from the sounding frequencies may also be retained as part of a ‘passive’ spectrum. As a consequence, whenever a sounding sweep is complete, both a sounding spectrum and a passive spectrum may be available. In addition, provided the retained passive bins (again usually 6 bins, 162.8 Hz in bandwidth) are those whose frequencies are the same as the ones that will be covered, by the next transmitting pulse frequency, i.e. in the next frequency step of the current sweep, the time delay, for a given frequency, between passive and sounding measurements becomes very short (less than 40 ms).

The WHISPER relaxation sounder has been designed in order to avoid, or at least minimize, any corruption between natural and sounding measurements, and also between sounding measurements. In particular, transmitted frequencies are swept in appropriate orders, described in tables chosen by command, in such a way that several consecutive transmitting pulses never have central frequencies close together. Passive measurements associated with sounding measurements are therefore not

influenced by long lasting resonances and no perturbations are expected between two successive sounding steps.

Analysis on the ground of the resonance pattern observed in active spectra (plus comparison with the associated passive spectra when available) allows the identification of characteristic frequencies of the surrounding plasma (see Section 12.4.1 and 12.4.2), in particular the plasma frequency  $F_{pe}$ , and hence the total electron density  $N_e = F_{pe}^2/\alpha$  where  $\alpha$  is a constant:  $\alpha = e^2/(4\pi^2\epsilon_0 m) = 80.7 \text{ Hz}^2/\text{cm}^3$ .

The sounding mode is operated alternately with the natural wave mode, with all four spacecraft following closely the same time line. Typically, 3 s (or 4 s) of sounding mode (two sweeps in frequency) are followed by 49 s (or 100 s) of natural wave mode, leading to a standard 52 s (or 104 s) sounding recurrence time. After September 2003, C4 CLUSTER spacecraft operates always at a 104 s sounding recurrence. In the standard (most frequently used) sounding cycle, the four spacecraft sound simultaneously every 104 s, and C1, C2 and C3 also sound 52 s later, but C4 does not transmit, it continues to monitor natural waves. Such a duty cycle is used for all WEC operations, both in nominal (NM) telemetry mode and in burst (BM) mode, when the time resolution of natural wave measurements is, on average, improved by a factor 5.

WHISPER data are usually presented in the form of dynamic spectrograms, in which the electric-field intensity is plotted as a function of time (abscissa) and frequency (ordinate) using a colour code. The spectrograms bear important information about explored regions. The characteristic signature of natural or actively triggered waves indicates the nature of the ambient plasma regime and, combined with the spacecraft position, reveals the position of key magnetospheric boundaries encountered during a specific time interval. Fig. 12.1 shows typical signatures encountered by CLUSTER. The yellow ellipses indicate natural emissions: (a) faint escaping non-thermal continuum radio waves, (b) continuum enhancement [8], (c) Type III solar radio burst and (d) magnetosheath low frequency turbulence. White arrows show characteristic resonances triggered by the sounder: (1) the plasma frequency

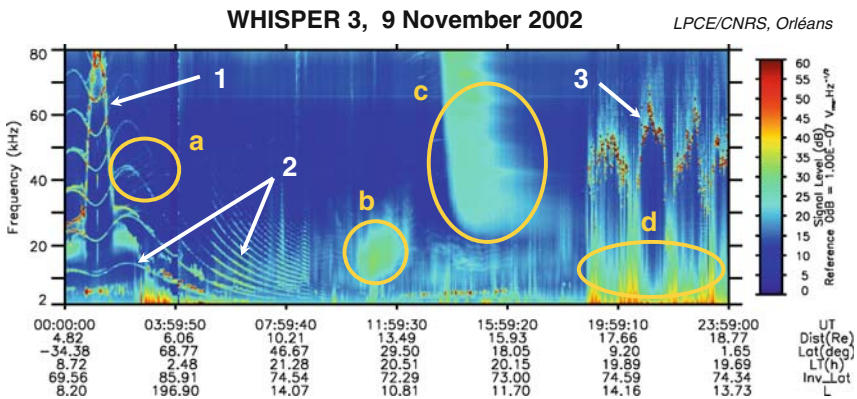


**Fig. 12.1** One day E-field spectrogram showing typical signatures of natural waves and resonances seen by the CLUSTER/WHISPER relaxation sounder (see text)

at the plasmopause boundary, (2) the electron gyrofrequency and its harmonics and (3) the plasma frequency in the magnetosheath. The plasmopause is recognized by the plasma frequency increasing as the spacecraft enters the plasmasphere near 00:50 UT, then decreasing near 01:50 UT as it exits. The magnetopause position (crossed at  $\sim$ 18:50 UT) is indicated by a rapid change in both the plasma frequency and the level of low frequency turbulence.

## 12.3 WHISPER Data Products in CAA

This section describes the WHISPER data products to a level adequate to be able to understand and start using them. Further information may be found in the CAA Interface Control Document for WHISPER [13], and other documents available on the CAA site.

All WHISPER data products are validated at LPC2E (Laboratoire de Physique et Chimie de l'Environnement et de l'Espace Orléans, France) before being delivered to the archive as CEF files (CLUSTER Exchange Format). Eleven WHISPER datasets are archived at CAA. They fall into four categories: natural waves (one science and one support dataset), energy (two science datasets), electron number density (one science dataset), and sounding (three science and three support datasets), as explained in the following sections.

### 12.3.1 *Natural Waves Related Datasets*

Most of the time WHISPER observes natural waves in the (2, 80 kHz) band, using one of the two EFW antenna pairs: Ey or Ez. Frequency spectra are obtained by onboard FFT (generally in 512 or 256 frequency bins, but 64 and 128 bins are also possible) with a nominal resolution of 162.8 Hz in 512 bins. Only accumulated bin moduli are transferred to the telemetry. Three gains are available: 12, 24, 36 dB. The 24/12 and 36/24 modes switch automatically from high gain to low gain whenever too many overflows are encountered, overflows being signal samples exceeding the dynamical range of the analog-to-digital converter. Natural wave spectra cannot all be transferred due to TM limitations: compression and selection are therefore required. A number of successive spectra called “average number”, are accumulated bin by bin, and accumulated spectra are transmitted at a rate selected to optimize the use of the TM rate available at the time. Finally, spectral values are compressed logarithmically from 24 bits (DWP word size) to 8-bit or 6-bit words. There are two types of natural wave related datasets: CP\_WHI\_NATURAL for natural (accumulated) spectra and CT\_WHI\_NATURAL\_EVENT indicating processing mode changes. Only the first is briefly presented below. The second is an event table, which contains engineering parameters needed to fully understand the associated physical data: for a description please refer to the ICD (2009).

CP\_WHI\_NATURAL files contain: the spectrum (central) time; the time uncertainty which is due to accumulation, in s; the FFT size; the EFW receiving antenna actually used; the electric-field spectral power densities computed on ground from accumulated moduli, expressed in  $V^2 m^{-2} Hz^{-1}$ ; the FFT bin frequencies, given in kHz; an overflow coded value which can vary between 0 (no saturation, i.e. no time samples out of limits before A/D conversion) and 1 (all time samples are out of limits, thus clipped during conversion); the average number, i.e. the number of accumulated spectra; the number of gain changes during acquisition; and the mantissa and exponent sizes of compressed data (usually adjusted to the observed signal dynamical range), which indicate the uncertainty in spectral line moduli due to onboard compression. It is important to recall that electric-field spectral power densities are not quantities directly delivered by the instrument, but are elaborated on ground. We will now follow each step of the conversion from TM words to physical quantities, in order for the user to appreciate the precision and reliability of the data.

The parameter measured onboard is the potential difference between the two probes used to form the dipole antenna, which is then analysed spectrally by FFT of successive segments of the waveform, the moduli of the complex Fourier transform being accumulated bin by bin to obtain the values transmitted to the ground. A telemetry word (of 6 or 8 bits) allocated to a bin is divided into two parts, the exponent and the mantissa. Their respective size (for instance 4 bits for the exponent and 2 bits for the mantissa) is the same for all words in the spectrum. Exponent indicates the dynamical range of a bin modulus in a given spectrum. For instance a value of 4 indicates that the number of bit shifts from the largest to the smallest values need 4 bits to be coded, meaning that all values are within a 96 dB range, which accommodates the largest dynamical range possibly encountered in the WHISPER instrument. The mantissa bit size gives the number of significant bits allocated to each bin modulus, thus the uncertainty; for instance a value of 2 yields an uncertainty below 25%. When the dynamical range of bin moduli is small, the exponent size is small (for instance, 2 bits for a range of 18 dB) and the mantissa size allows a high precision (a 4 bits mantissa leads to an uncertainty below 6%). The shift value common to all bins, i.e. the position of largest shift, is indicated via the bin size information (exponent and mantissa sizes) present in the data record of each spectrum.

The receiver transfer function (gain in modulus versus working frequency) is known with a similar uncertainty, of order 1 dB, to what is due to onboard compression. The transfer function has been measured on ground with great detail, on each spacecraft and in various environmental conditions. A possible evolution of this quantity exceeding tolerable thresholds would immediately be known to the WHISPER operation team, via results of onboard calibrations activities, run every orbit. Nothing of the kind happened since the start of CLUSTER mission. The same calibration functions have thus been applied on ground since then, translating telemetry words to physical quantities. The total uncertainty attached to the electric field spectral modulus is estimated to be about 2 dB.

To determine the electric field, i.e. the physical quantity of interest, the potential difference must be divided by the effective (electrical) length of the antenna. The latter has been assumed to be equal to 100 m tip-to-tip which is the rounded

geometrical length (actually 88 m). While the geometrical length is used widely to convert potential differences to electric-field values, it is only a crude approximation of the effective length. It may be indeed significantly wrong close to characteristic frequencies of the ambient plasma, and possibly too in conditions, natural or instrumental (EFW), which produce an unusual plasma sheath around the antenna. This point is discussed further in Section 12.6. The final operation transforms the electric field spectral moduli to the equivalent spectral power density, while simultaneously taking account of the shape of the Blackman-Harris windowing function applied prior to FFT analysis.

### ***12.3.2 Energy Related Datasets***

In each natural spectrum acquisition interval, the large band (2–80 kHz) electric potential is sampled over 512 or 1024 time samples (depending on FFT size) which are squared, summed, and transmitted. A compression from 48 to 8 bits is applied onboard, with fixed bit allocations for the exponent and for the mantissa. The dynamical range of the energy parameter, corresponding to the ratio between the largest and smallest measurable values of large band electric-field power, is only 48 dB, due to instrumental limits. The energy parameter is thus especially interesting in case of bursty signals of large amplitudes, and when the selection rate of transmitted spectra is severe. In such cases, it allows to survey the variability of the electric field during the time intervals when spectra are not transmitted. There are two datasets related to ‘energy’ like parameters: CP\_WHI\_WAVE\_FORM\_ENERGY; and PP\_WHI. The latter gives, together with an extremely crude estimate of density, the energy in three wide frequency bands (2–10, 10–20, and 20–80 kHz), calculated on ground from available spectra, and the normalized standard deviation of large band electric field power from time samples, calculated on ground.

### ***12.3.3 Sounding Related Datasets***

As for the natural wave spectra described in Section 12.3.1 not all the active/sounding spectra can be transferred due to TM limitations: compression and selection are thus required. Different strategies can be selected such as: compression of the values (to 8-bit or 6-bit words); reduction of the frequency sweep range; active bins grouped by pairs, with only the greater of each pair being kept, and the missing spectral values being filled by linear interpolation during ground processing prior to archiving; active-to-passive ratios coded on 2 bits and transmitted rather than sending passive data.

As described in Section 12.2, whenever a frequency sweep is complete, both an active spectrum and a passive spectrum are available. They are constructed with frequency bins selected in each of the frequency steps that compose the sweep, so that



the time difference, for a given frequency, between a passive bin and an active bin is less than 40 ms. Let us recall that passive spectra have a frequency/time distribution which is significantly different from that obtained in the natural wave modes described in Section 12.3.1. The constructed ‘passive’ spectrum associated with the ‘active’ spectrum can be sent to ground or used to compute active-to-passive ratios that can also be sent to ground, depending on the chosen compression strategy. Comparison of ‘passive’ and ‘active’ conditions at a given frequency during a single frequency sweep is possible because the succession of the frequency steps in a sweep are ranged in such an order as ‘passive’ measurements cannot be perturbed by previous soundings (see Section 12.2). This is a great advantage compared to previous sounder concepts, because the time delay between these passive measurements and the related active ones is here very short (a few tens ms instead of a few s). The 2-bit coding of the active-to-passive intensity ratio is as follows: if  $(\text{active}/2 \leq \text{passive})$  return 0; else if  $(\text{active}/4 \leq \text{passive})$  return 1; else if  $(\text{active}/16 \leq \text{passive})$  return 2; else return 3).

The types of sounding related archives are six in number:

- CP.WHI.ACTIVE including sounding (active) spectra
- CP.WHI.PASSIVE\_ACTIVE for associated passive spectra
- CP.WHI.ACTIVE\_TO\_PASSIVE\_RATIO, which contains the active to passive ratios (with only four possible values for each bin)
- CT.WHI.ACTIVE\_EVENT to list sounding mode changes
- CP.WHI.HK, which gives elementary sounding events extracted from the WEC housekeeping files
- CP.WHI.SOUNDING\_TIMES, which is a simplified version of the above mentioned CP.WHI.ACTIVE file where only the sweep central sounding time is kept

The CP.WHI.ACTIVE content is recalled below, for the other files please refer to the ICD for WHISPER document (2009). In the CP.WHI.ACTIVE file, we find the following information: spectrum (central) time; time uncertainty due to acquisition and sweep, in s; the EFW receiving antenna used; the active electric-field spectral power densities, in  $\text{V}^2 \text{m}^{-2} \text{Hz}^{-1}$ ; FFT bin frequencies, in kHz; scanned frequency table, which gives the transmitted frequencies and the sweep order; sounding pulse length, in ms; time between 2 successive emissions in a sweep; emission/reception delay i.e. the time between emission and reception; number of gain changes; and compression parameters i.e. the mantissa and exponent sizes.

### ***12.3.4 Electron Density Related Dataset***

Compared with the three previous categories of WHISPER data products, created at CNES, validated at LPC2E, and directly delivered by CNES to CAA, the CP.WHI.ELECTRON.DENSITY file is not a product which can be generated by routine processing (decommutation and conversion into physical units) of WHISPER data. As explained in Section 12.4, the electron density is determined from either the characteristic plasma frequencies at which resonances are triggered when

WHISPER is in sounding mode, or from natural wave signatures, or a combination of both [Chapter 18 of this book, 22, 24]. Density files result from complex procedures which require human intervention and scientific expertise, and therefore they are produced at the laboratory and delivered to CAA on a best effort basis.

Are included in the CP\_WHI.ELECTRON.DENSITY file: the central time of the spectrum from which the density is derived; the uncertainty time, in s; the spectrum type (Active or Natural); the computational method, i.e. the algorithm and code used; information on the external data used, for example E whenever EFW data are used; the derived electron density value, expressed in  $\text{cm}^{-3}$ ; the electron density uncertainty, expressed in  $\text{cm}^{-3}$ , if available (depends on the applied algorithm); a “contrast” factor, between 0 and 1, if available (based on the local contrast of the peak/cut-off, as we will see later).

## 12.4 Electron Density Determination Process

The electron density is determined semi-automatically with the help of a specific tool called FPTool whose working principle is shown in Fig. 12.2. The first step is to visualize input parameters from the four spacecraft, such as the WHISPER active/passive spectrograms, the EFW spacecraft potential and FGM magnetic-field strength. The user is then invited to select a frequency band that includes the plasma frequency signature, a resonance or a clear cutoff, from which the density will be derived [25]. Knowledge of the region (plasma regime) where the spacecraft is located is also highly desirable for a reliable determination; this information may come from the ESOC Predicted Event Times or the dedicated software (MAGLIB) developed at CNES. The next step is to choose and apply the appropriate algorithm (FPTool box in Fig. 12.2) to look at the electron density file (Fp file box in Fig. 12.2) that

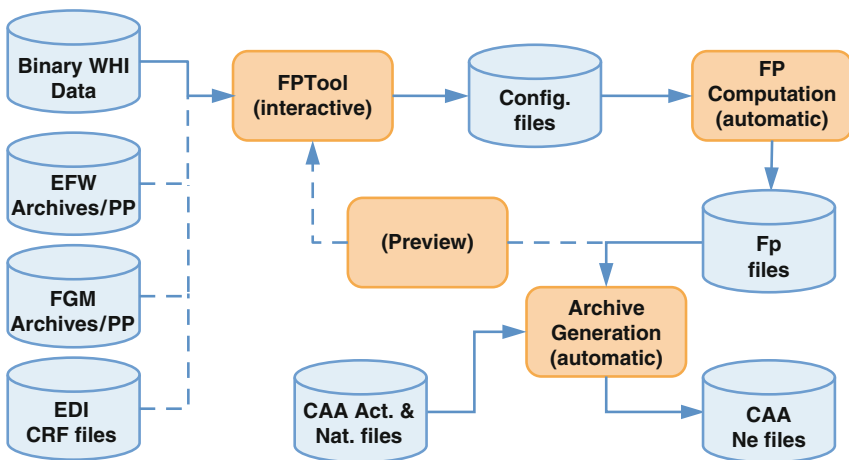


Fig. 12.2 FPTool flow chart describing how the CAA WHISPER density files are produced

is produced and, if necessary (Preview box in Fig. 12.2), remove erroneous values or select another algorithm. The loop indicated in Fig. 12.2 (FPTool – FP Computation – Preview) is driven until a satisfactory result is obtained. This process has been conceived to minimize large errors in the density estimate, to confirm that the most appropriate algorithm has been applied, and to minimize the time necessary to validate products automatically created.

### ***12.4.1 Density Determination in the Solar Wind and Magnetosheath***

Only one strong resonance is usually observed at, or close to, the plasma frequency  $F_{pe}$  from which the density  $N_e$  is directly derived (see also Section 12.2):

$$N_e[\text{cm}^{-3}] = F_{pe}^2[\text{kHz}]/80.7$$

In addition, lower cut-off of thermal noise recorded whenever WHISPER is used as a natural wave detector is also a valuable way to determine  $N_e$ . Cut-off indeed occurs very close to  $F_{pe}$ . Another way to derive  $N_e$  is to combine WHISPER active observations with S/C potential measurements made by EFW and to adjust, at best, the two time series, interval by interval. Pattern recognition processes are therefore applied.

Thus, the density (plasma frequency) determination process may be decomposed into three steps: a preprocessing of active spectrograms; a reliable identification of plasma-frequency resonances on active spectra (only peaks with high signal-to-noise ratios are kept); and finally a density extraction from active and/or passive spectra in a frequency band centered on the general trend of the plasma frequency variations. This trend is defined using the previously determined resonance frequencies and interpolation frequencies coming from any cut-off signature and/or a recalibration of the EFW S/C potential. It is worth noting that some of the resonances that were first rejected due to their low signal-to-noise ratios may be finally reselected provided they are in the search frequency band. The two last steps are illustrated in Fig. 12.3.

The active spectrogram pre-processing consists in removing the interference signals (perturbations from EDI, spurious signals from the onboard power converter, or DSP bug in the FFT transform for WHISPER). These signals are detected by converting active spectrograms into “peak images” where only spectral peaks are kept [19]. A morphological “opening” operator is applied on the obtained binary images along the “time” dimension. Whenever three peaks are at least located at the same frequency in five contiguous spectra, they are considered as interference signatures, and the five values related to this frequency are then removed and replaced by interpolated values.

How to compute the plasma frequency from active spectra?  $F_{pe}$  is usually characterized by a strong resonance. It is therefore given by the tallest peak in each

WHISPER 1, 06 June 2002, Earth's Magnetosheath

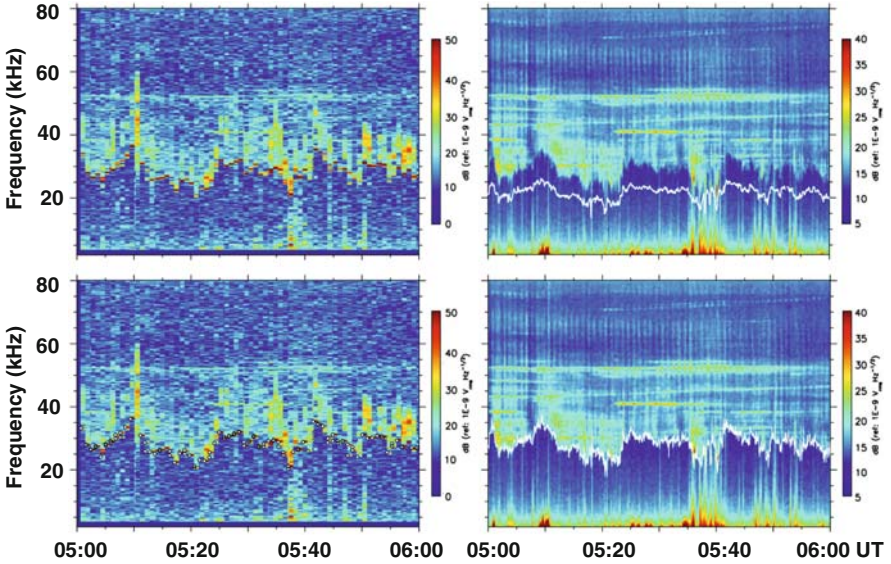


**Fig. 12.3** Density determination in magnetosheath: *top-left panel*, WHISPER active spectrogram; *bottom-left panel*, identified plasma frequency resonances (*white full circles*) superimposed on active spectrogram; *top-right panel*, plasma frequency derived from the EFW S/C potential (*white line*) superimposed on WHISPER natural/passive spectrogram; *bottom-right panel* plasma frequency (*white line*) deduced from natural wave lower cut-off superimposed on passive spectrogram

spectrum, provided its intensity (in dB) is at least 0.85 times higher than the intensity (in dB) of the second tallest peak. The  $F_{pe}$  uncertainty is nominally 163 Hz, the best WHISPER frequency resolution. The values obtained are shown in the lower left panel of Fig. 12.3. The “contrast” factor, which is also given in the dataset, reflects the local contrast of the peak. Let  $P$  be the tallest peak intensity relative to the background level and  $M$  the mean intensity in the 20 frequency bins around the peak, the contrast factor  $C$  is simply given by:

$$C = \min(P / M - 1, 1)$$

The last step in this example is the use of cut-off signatures and/or EFW S/C potential recalibration. A rough approximation of  $F_{pe}$  may indeed be derived from the S/C potential  $SP$  (which is negative) using the empirical relation:

$$F_{pe} = 9(\alpha(-SP)^\beta)^{1/2},$$

with, by default,  $\alpha = 200$  and  $\beta = -1.85$  (if necessary, these values can be adjusted by the operator during the validation process). The resultant  $F_{pe}$  curve is then fitted to the above mentioned extracted resonances by a simple affine transformation. There are now two possibilities: whenever a clear cut-off arises in natural/passive

spectra, its frequency is automatically extracted inside a search band (about 30 frequency bins in width) defined around a  $F_{pe}$  curve that links up the already extracted resonances or the  $F_{pe}$  curve coming from the S/C potential recalibration; conversely, if no natural signature is present at all, the EFW fit itself is given as the plasma frequency. Let us note that the contrast factor is set to the fill value of  $-1$  when the density value is obtained from EFW data. Otherwise, the contrast is an indicator of the contrast of the low cut-off range in the search band. Let  $M$ ,  $U$ , and  $L$  be the mean signal magnitudes in respectively, the whole search band, the upper part of the search band (from the cut-off frequency bin returned by the algorithm to the upper limit of the search band), and the lower part of the search band (from the lower limit of the search band to the cut-off frequency bin returned by the algorithm), the contrast factor  $C$  is given by:

$$C = \max(\min((U - L) / M, 1), 0)$$

Finally, it may be noted that the cut-off seen in the natural wave spectrograms of Fig. 12.3 is that of the continuum which differs from the thermal noise that has a much narrower bandwidth, within which there is no structure. The fact that the cut-off is close to the plasma frequency can be confirmed here by comparison with the plasma frequency resonances shown in the bottom left panel, this is a great advantage compared with only passive experiments: natural waves may be indeed generated at a considerable distance from the spacecraft and their frequency signatures, such as cut-offs, may thus not reflect local plasma characteristics. Let us also note that in the solar wind and magnetosheath the electron gyrofrequency  $F_{ce}$  is too low compared with the plasma frequency  $F_{pe}$  for the upper-hybrid frequency  $F_{uh}$  (if actually triggered) to be distinguished.

#### 12.4.2 Density Determination in the Plasmasphere, Cusp and Tail

In the Earth's magnetosphere, and in particular in the plasmasphere, resonances arise at the electron cyclotron frequency  $F_{ce}$ , its harmonics  $nF_{ce}$ , the electron plasma frequency  $F_{pe}$ , the upper-hybrid frequency  $F_{uh}$  ( $F_{uh} = (F_{pe}^2 + F_{ce}^2)^{1/2}$ ), and  $F_{qn}$  that correspond to Bernstein electrostatic cyclotron waves with group velocity close to zero ( $F_{qn} > 2F_{ce}$  and  $nF_{ce} < F_{qn} < (n + 1)F_{ce}$ ). A detailed plasma diagnosis can therefore be made from the identification of these resonances, which depend on the magnetic field strength and the total electron density. Two populations of electrons, cold and hot may also be revealed [23]; nevertheless this kind of analysis is too intricate and time consuming to be performed automatically. Consequently, we decided to take advantage of the higher spectral energy density close to  $F_{uh}$ , from which the plasma frequency (and thus the electron density) may be directly derived. It has been indeed established from many observations in the magnetosphere (on ISEE-1 GEOS 1 & 2, Viking) that the resonances, including the  $nF_{ce}$  series, are more intense close, and above, the plasma frequency and that the spectral energy

density reached its maximum very close to  $F_{uh}$  [11,21]. The magnetic field strength, and hence  $F_{ce}$ , are known either from FGM or from  $nF_{ce}$  observed by WHISPER ( $F_{ce} = 28 B$ , where  $F_{ce}$  is expressed in Hz and  $B$  in nT).

Active spectrograms are first pre-processed to enhance the contrast of resonances: a morphological top-hat operator [20] is first applied to each spectrum and spectra are not normalised [19]. In other words, as usual in image processing the objective is to reduce the noise and to detrend the image while preserving edges in order to highlight peaks. Spectra are then smoothed (Butterworth filter) and the peak frequency of each smoothed spectrum is retained as  $F_{uh}$ , the uncertainty being the half-width at the half-height of smoothed peaks. Let also note that only maxima with intensities at least five times higher than the around background level observed in close natural/passive spectra (10 frequency bins around) are retained. Are also discarded spectra where two or more peaks are observed with similar intensities. The kept points are indicated in green and those who are rejected in black, in the bottom-left panel of Fig. 12.4 The next step is the EFW S/C potential recalibration on the “green” points as described in Section 12.4.1. A search band may then be defined around the obtained  $F_{uh}$  values (the upper and lower limits of this frequency band, shown as red lines in the bottom-left panel of Fig. 12.4, are respectively 0.5 and 1.5 times these values derived from the recalibrated potential). Finally, a new

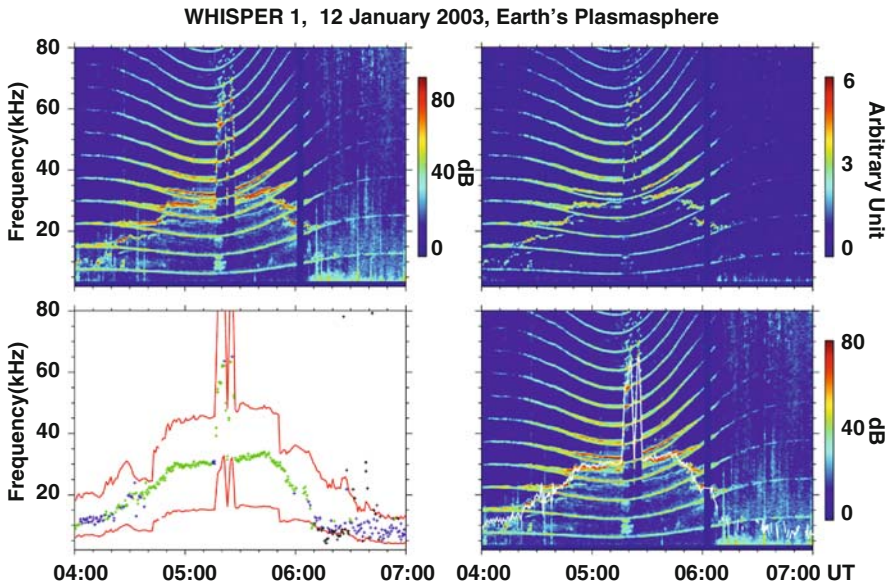


**Fig. 12.4** Upper-hybrid frequency  $F_{uh}$  determination in plasmasphere: *top-left panel*, WHISPER active spectrogram; *top-right panel*, reprocessed active spectrogram to bring out resonances; *bottom-left panel*, search band (red lines) around the  $F_{uh}$  calculated from the re-calibrated EFW density estimate,  $F_{uh}$  derived from WHISPER resonances (points kept during the first recognition step in green, rejected points in black, new points obtained during the last step of the recognition process in blue); *bottom-right panel*, final set of identified  $F_{uh}$  (white line) superimposed on active spectrogram

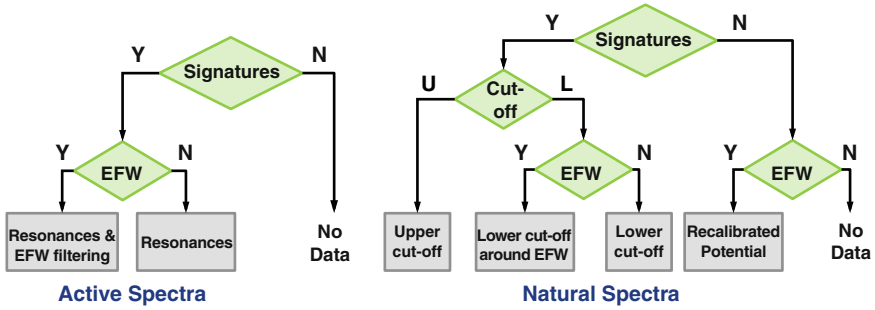


Fig. 12.5 Flow charts of plasma frequency/density recognition algorithms that are applied to WHISPER active (on the right) and natural/passive (on the left) E-field spectra, depending on the availability of EFW S/C potential data and upper or lower cut-off signatures of natural waves

search of spectrum maxima is made in this frequency band, which gives the final set of  $F_{uh}$  values: they are represented in green and blue. The last step of processing calculates  $F_{pe}$  from the pair  $F_{uh}$  and  $F_{ce}$ , and finally the density.

Figure 12.5 shows the different strategies that can be used to determine the electron density, depending upon the available inputs: resonances, natural wave cut-off signatures, and EFW spacecraft potential measurements. It applies to all plasma regimes.

## 12.5 Cross-calibration Activities

WHISPER determines the total electron density from the propagation characteristics of radio waves in a large region of space surrounding the spacecraft, and consequently the satellite potential and the plasma sheath surrounding the spacecraft have negligible effect on the measured density. The PEACE experiment measures the flux of electrons at down to thermal energies, where the correction for the spacecraft floating potential is significant. Therefore there is a strong demand from PEACE for high reliability electron density data from WHISPER, which regularly receives lists of time intervals of particular interest. As these intervals are well in advance of the foreseen WHISPER date for delivering these data to CAA, it was agreed not to interrupt routine WHISPER density production, but to provide for PEACE cross calibration work specially derived accurate and reliable density files which, for convenience, are in a simple ASCII format. The main problems arise from the fact that the requested time intervals, particularly in the cusp and tail regions, are often difficult to interpret and process due to the absence of triggered resonances, the absence of clear signatures in the natural/passive data, and/or strong interferences of various natures. Anyway, the process is not without success and PEACE still continues to ask for new time intervals.

For cross-calibration of the magnetic field with FGM and EDI resonances observed by WHISPER in the plasmasphere have been used. These resonances occur

at the electron cyclotron frequency  $F_{ce}$  and its harmonics  $nF_{ce}$ , from which the magnetic field strength may be derived (see Section 12.4.2). An algorithm has been developed [19], leading to a sub-pixel accuracy for the  $F_{ce}$  determination, i.e. less than 163 Hz, the highest WHISPER frequency resolution. It is based on the Radon transform technique, commonly used in image processing. This algorithm has been validated on synthetic spectrograms. WHISPER measures  $F_{ce}$  (and hence the magnetic field strength) directly, and the only limitation comes from the measurement accuracy. By using the  $nF_{ce}$  the  $F_{ce}$  determination can be much more accurate provided the number of available harmonics is sufficient.

Particle instruments have great difficulty in analyzing particle fluxes at thermal energies, which are comparable with the spacecraft floating potential. WHISPER should be of great help for internal calibration of such measurements. Particular attention has therefore to be paid to comparing density evaluations from WHISPER and CLUSTER particle experiments. The same is true for EFW and WHISPER density products [16].

## 12.6 Discussion and Conclusion

The WHISPER relaxation sounder has been designed in such a way that natural wave (passive) and even active measurements cannot be perturbed by long lasting echoes received after transmitted wave trains. We indeed know, since the eighties, that sounder-stimulated resonances can last up to a few 100 ms (see, for example, Figure 12.2 in [21]), it is therefore required not to perform any natural and even active measurements at, or close to, the same frequency of the last transmitted pulse before the echo intensity fades away. To solve this problem, natural wave measurements are always made before active measurements and in active modes the transmitted frequencies are not swept in a regular order, they follows an appropriate order, which is described in a table and chosen by command, where two successive frequencies are always well separated. Finally, let us note that the minimum time separation between WHISPER active and passive operations is 215 ms, i.e. the time separation between the last sounding pulse and the next natural waveform recording: so even for very long lasting resonances no perturbations may be detected on natural spectra due to the averaging process applied before TM delivery.

One appreciable advantage of WHISPER instrument, shared by most wave instruments, is that calibration files are stable over the mission lifetime. Conversion of raw spectra to physical units can be performed at an early stage of data handling, immediately after telemetry decommutation. The calibration procedure is still executed once per orbit, to check the instrument's health. But during the 8 years since launch, the calibration files have never needed any revision. We may note that amplitudes of waves from distant radio sources (type III solar bursts), as measured from the four different WHISPER instruments, are equal to within 1 dB, less than the experimental uncertainty which is estimated to be 2 dB. Furthermore, the conversion of bin number to frequency is well defined due to the high stability of the onboard oscillators, and does not evolve with time.



However, a word of caution must be given concerning signal amplitudes. To convert the potential difference measured by the antenna to an electric field a fixed effective antenna length has been used. In reality, the CLUSTER antenna effective length depends on the plasma regime (see [1]). Scientific studies requiring precise signal amplitudes may need a better estimation of the antenna effective length as, for example, in the study of electrostatic waves as a possible cause of the precipitation of the particles associated with diffuse auroras [9].

The intrinsic quality of the main WHISPER data products (high resolution electric-field active/passive spectra, power spectral density, and large band intensity) is considered to be good, except when: (1) There are gaps in the data from one or more of the spacecraft during segments of the orbit where data coverage had been planned (as indicated in the Master Plan). Some gaps affect easily identifiable time intervals, other are irregular and random; (2) WHISPER data are corrupted on one or more spacecraft, possibly due to DWP/EFW/WHISPER bugs; (3) EDI strongly perturbs WHISPER data. EDI Event files indicate time intervals that are potentially affected, and the probable extent of the perturbation.

The quality control of WHISPER density products is performed during the production of the plasma frequency. If the plasma frequency determination seems flawed it is corrected when possible, or else discarded. An automatically-computed “contrast” index is associated with each determination (see Section 12.4.1, for example). Examples of contrast factors for density determinations from active and passive data respectively are shown in Figs. 12.6 and 12.7. As  $F_{uh}$  resonances shown in the

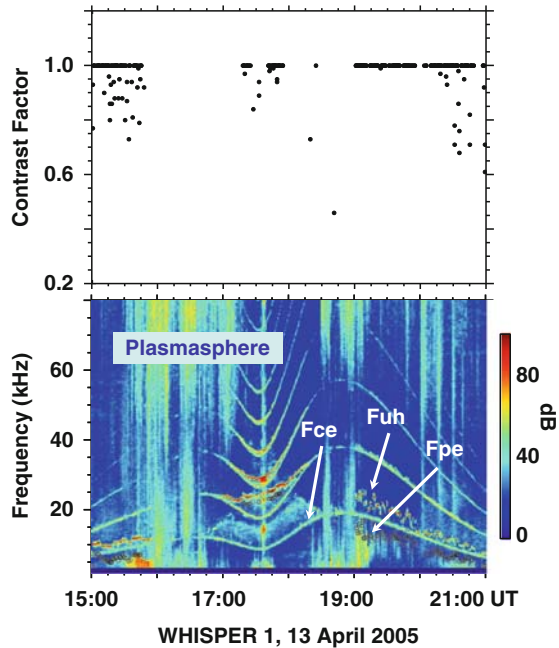


**Fig. 12.6** Example of the contrast factor associated with the density derived from WHISPER active measurements in the plasmasphere: *bottom panel*, the derived plasma frequency (*white full circles*) superimposed on WHISPER combined active/passive spectrogram; *top panel*, the associated contrast factor computed during the recognition process

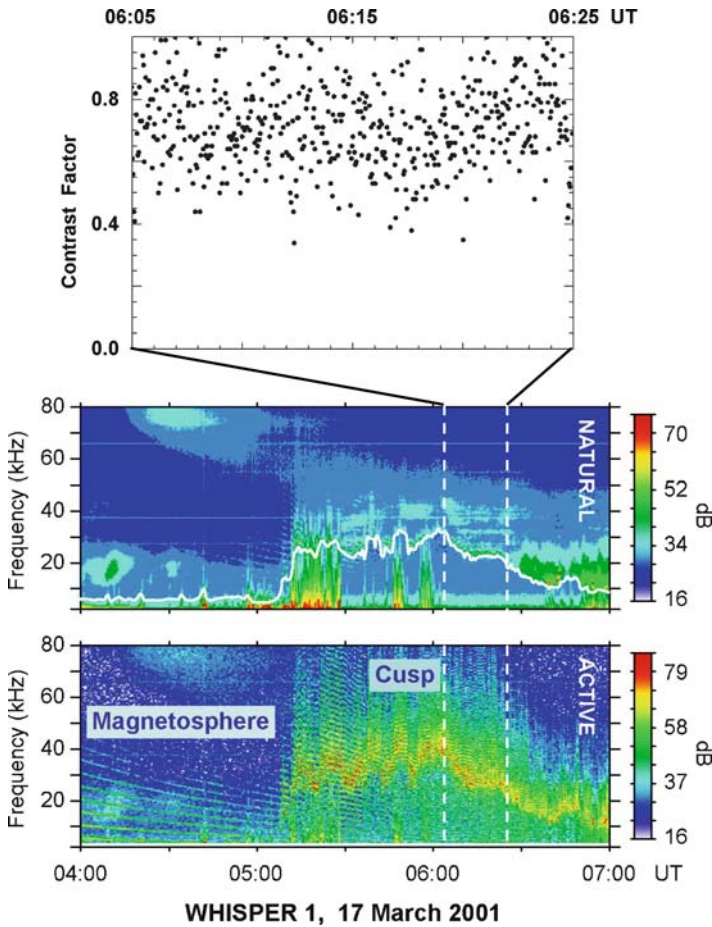


**Fig. 12.7** Example of the contrast factor associated with the density derived from WHISPER passive/natural measurements in the cusp region: *bottom panel* active spectrogram; *middle panel* plasma frequency (white line) superimposed on natural spectrogram; *top panel*, the associated contrast factor computed during the recognition process

bottom panel of Fig. 12.6 are, in this plasmasphere event, strong monochromatic peaks compared with the surrounding background level, the recognition process worked satisfactorily. The derive plasma frequencies are represented as white full circles in the active spectrogram (bottom panel) of Fig. 12.6 and, as can be seen in the top panel, the computed density contrast factors are very high. Figure 12.7 is an example of density determination results in the cusp region. Here the natural wave cut-off (middle panel) and resonances (bottom panel) were both used to obtain the plasma frequency profile shown as a white line in the natural spectrogram (middle panel). The contrast factor of density values derived from natural wave cut-off signatures, between 06:05 and 06:26 UT, is given in the top panel of Fig. 12.7.

Although the latter density values are very close to those derive from resonances, the contrast factor values appear to be equally distributed between 0.4, the value of the threshold used here, and 1.

If the plasma frequency is found to be too “noisy” the user can either check the contrast factor and plasma frequency uncertainty and possibly remove unreliable values, or keep only density values derived from active spectra, with a consequent lower time resolution. It is worth recalling that electron density files are high level products that require human intervention and scientific expertise, their production is time consuming, and therefore they are produced and delivered on a best efforts basis. Anyway, the policy is to give as complete and as good a dataset as is possible.

Two frequently asked questions are:

- What is about the density determination in non-maxwellian plasmas, such as a bi-maxwellian with 10 eV and 10 keV populations?
- What are the connections with the boom and Debye lengths?

To tentatively answer the first question we can consider the Earth’s plasmasphere where two series of Bernstein  $F_{qn}$  resonances are often observed (two resonances instead of one are seen between two successive gyroharmonics, see for example Fig. 12.8 in [22]). Theoretical calculations [2] have shown they may be explained by the presence of a hot electron component superimposed on the dominant cold one. One of the two observed  $F_{qn}$  series is aligned in an appropriate plot, the so-called Hamelin diagram (The frequency separation between a  $F_{qn}$  and the gyrofrequency  $nF_{ce}$ , that is just below, is plotted as a function of the plasma frequency). This series is due to the cold plasma component and the corresponding density may therefore be simply deduced from the plasma frequency read on the plot abscissa. The other series can be used to estimate the hot to cold density and temperature ratios. The total density which can be derived in this way – after a time consuming analysis – is generally not very different from the density of the cold population. We consider nevertheless that the parameter to be archived is the total density. Hopefully, additional resonances related to the total density are often detected: one is the so-called  $F_x$  [2], which turns out to be the total electron plasma frequency here, the other is the upper-hybrid frequency  $F_{uh}$ .

In the solar wind and magnetosheath  $F_{pe}$  and  $F_{uh}$  almost merge due to the weak intensity of the embedded magnetic field, leading to a single resonance observed in the active spectrum. There is thus no risk of a wrong identification of the characteristic plasma frequency, except in case of significant spurious noise, which is taken care of as explained in Section 12.4.1: in case this risk is present, a contrast factor linked to each density determination would be significantly lower than 1. The uncertainty on the plasma frequency resonance being the FFT frequency resolution, usually 162.8 Hz, the accuracy of the total electron density is thus a few percents for low densities (4% for an electron plasma frequency  $F_{pe} = 9$  kHz, i.e. a density of  $N_e = 1 \text{ cm}^{-3}$ ) and less than 1% for high densities (0.5% for  $F_{pe} = 63.6$  kHz, i.e.  $N_e = 50 \text{ cm}^{-3}$ ).

In magnetized regions, like the plasmasphere, the resonance pattern is more complex. Resonances are indeed observed at  $F_{ce}$  (which is proportional to the magnetic

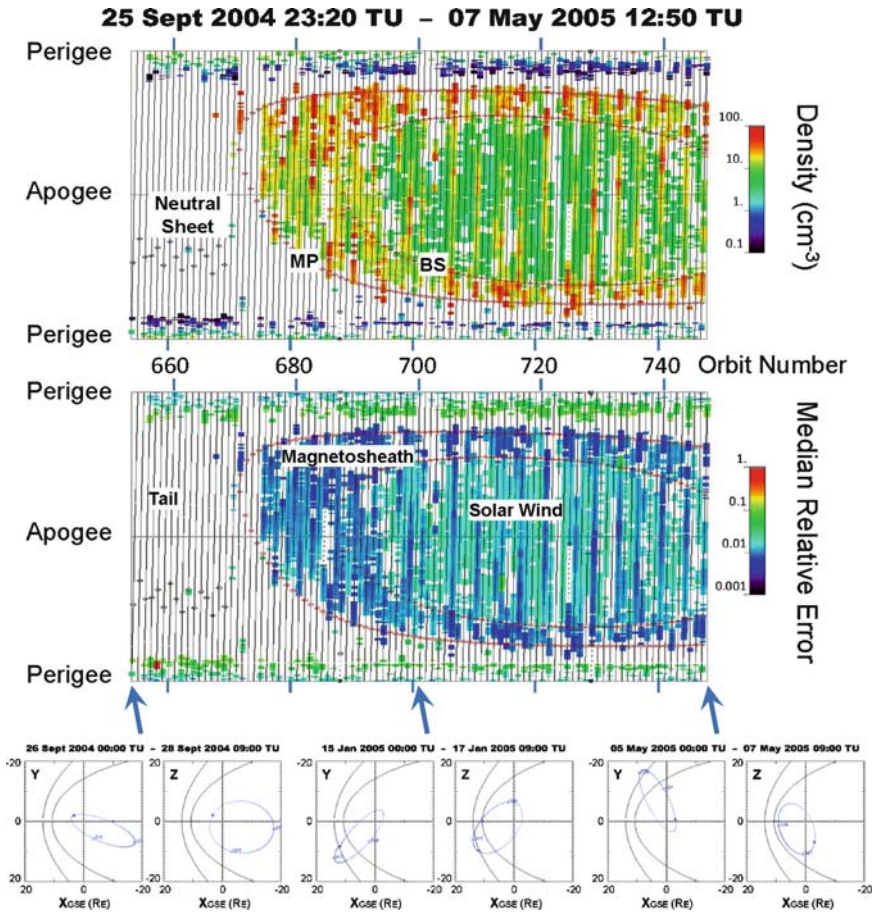


**Fig. 12.8** Bryant plots showing the averaged density (*top*) and its “accuracy/uncertainty” (*middle*) during almost 8 months. In Bryant plots, the horizontal axis is absolute time or orbit number while the vertical axis is time since last perigee; thus each orbit is represented by a sloping line. The reference S/C position is given at the beginning, middle, and end of the time interval (*bottom*)

field strength), its harmonics,  $F_{pe}$  (proportional to the square root of the electron density),  $F_{uh}$  (the square root of  $F_{pe}$  squared plus  $F_{ce}$  squared), and  $F_{qn}$  (which are higher than  $2F_{ce}$ , higher than  $F_{uh}$ , thus also higher than  $F_{pe}$ , and observed between two successive gyroharmonics). As said in Section 12.4.2, the challenge presented to the processing algorithm is the correct identification of  $F_{uh}$ , which is considered as the most intense and reliable resonance from which the total electron density may be derived,  $F_{ce}$  being computed either from FGM magnetic measurements or  $nF_{ce}$  resonance frequencies. Section 12.4.2 also explains how the algorithm works, identifying  $F_{uh}$  as the frequency at highest intensity in the smoothed active frequency spectrum. The  $F_{uh}$  value returned by the algorithm may unfortunately differ from the true  $F_{uh}$  (when recognized via the  $F_{pe}$ ,  $F_{uh}$ ,  $F_{ce}$  relationship). This is because the

amplitudes of the resonances that may be observed close to the computed smoothed spectrum maximum ( $F_{pe}$ ,  $F_{uh}$ , the first  $F_q$ , possibly double, and even gyroharmonics) vary with the actual plasma composition (hot to cold density ratio) and also with antenna orientation with respect to B-field orientation, such that the highest peak may be not always at  $F_{uh}$ . However our practical expertise, based on numerous detailed analysis of case event studies, indicate that most of those resonances are grouped within a not too large frequency interval in the regions explored by CLUSTER.

Diffuse plasma D resonances are currently observed in the ionosphere but have not been observed by the WHISPER relaxation sounder [24], probably due to the low level of the emitter.

A crude estimate of the uncertainty range linked to the density data obtained in a magnetized region can be provided. Let's take, as illustration, a case in the plasmasphere where  $F_{ce} = 10$  kHz. Whenever  $F_{uh}/F_{ce} < 2$ , the resonance observed between  $F_{ce}$  and  $2F_{ce}$  is  $F_{uh}$ , with a frequency resolution of 162.8 Hz, the FFT frequency resolution. The relative uncertainty on the density varies hence between  $+/- 30\%$  ( $F_{uh}$  near  $F_{ce}$ ,  $F_{uh} = 10.55$  kHz,  $N_e = 0.14$  cm $^{-3}$ ) and  $+/- 2.3\%$  ( $F_{uh}$  near  $2F_{ce}$ ,  $F_{uh} = 19.6$  kHz,  $N_e = 3.5$  cm $^{-3}$ ). In case  $F_{uh}/F_{ce}$  is in the range 4–6 and with a 2 kHz uncertainty on  $F_{uh}$  position ( $\sim 12$  frequency bins) leads to a density uncertainty from  $+/- 10\%$  ( $F_{uh}$  near  $4F_{ce}$ ,  $F_{uh} = 41.5$  kHz,  $N_e = 20$  cm $^{-3}$ ) to  $+/- 7\%$  ( $F_{uh}$  near  $6F_{ce}$ ,  $F_{uh} = 57.8$  kHz,  $N_e = 40$  cm $^{-3}$ ).

To summarize, the density which is archived can reasonably be considered to be the total electron density in all regions. The uncertainty about the density is primarily due to the FFT frequency resolution, except in magnetized regions, where it is usually below 10% (up to about 30% when  $F_{uh}$  is close to  $F_{ce}$ ).

Concerning the relative sizes of the wavelength  $\lambda$  of the excited waves and the length  $L$  of the physical antenna, we know that whenever  $\lambda$  is close to or shorter than  $L$ , the amplitude of the received signal varies as  $\lambda$  for spherical probes, and the signal fades if  $L$  is a multiple of  $\lambda$  [12]. However, waves excited by relaxation sounders are electrostatic in nature. Their wavelengths are therefore, most of the time, very large compared with the antenna length. Resonance frequencies are not affected.

On comparative sizes of the Debye length  $\lambda_D$  and the physical antenna length  $L$ , let us recall that the minimum wavelength in a collective plasma is actually  $\lambda_D$ , so the antenna must be longer than  $\lambda_D$  in order to sense the plasma presence instead of responding as if it were in free space. A hot population with an associated Debye length much larger than  $L$  could therefore be ignored by the sounder. Unfortunately, no quantitative estimate of the real limit has been made. However, qualitative information is available (comparison of the signatures of sounder and mutual impedance experiments, theoretical models of the mutual impedance response: [4, 5, 17]).

Let us finally mention that visualization tools have been developed to validate data a posteriori and to overview density products. Two outputs of one of them are presented in Fig. 12.8. The Bryant plot [14] format has been used to see the averaged density and its uncertainty over large time intervals. Predictions of various boundary crossings, including the neutral sheet, magnetopause and bow shock, are indicated

by coloured symbols. WHISPER operates in all regions but it becomes clear that the favourable regions for the density determination (i.e. where resonances are triggered in the instrument's frequency range at a high enough level and natural wave signatures, such as cut-offs, are observed and identified) are: solar wind, most of magnetosheaths, cusp and clefts, parts of dayside magnetosphere, parts of nightside plasmashet. Most of lobes are unfavourable.

As a conclusion, the sounder is certainly a sophisticated instrument, but it is robust and it produces data whose quality is both very stable over the long-term, and from which it is possible to derive, in most of the key regions of the Earth's ionized environment, reliable and accurate measurement of the total ambient electron density in a volume of space large enough for local plasma sheath effects to be negligible. Plasma densities (as archived in CAA) from 0.14 to 80 cm<sup>-3</sup> are derived from WHISPER relaxation sounder data with a good accuracy: a few percents for low densities and less than 1% for high densities, in non-magnetized or weakly magnetized regions; and, for instance, below 10% when  $F_{pe}$  is above 0.7  $F_{ce}$  down to about 30% when  $F_{pe}$  is close to 0.34  $F_{ce}$ , in magnetized regions with  $F_{ce}$  around 10 kHz). WHISPER densities are therefore currently used for calibrations of CLUSTER instruments, in particular particle instruments, which have difficulties to measure the colder part of the population, and EFW instrument, because spacecraft potential variations, currently used as a proxy of density variations, depend not only on the density but also on the energy of electrons. Finally, it is worth recalling that WHISPER also allows the spectral energy distribution of natural waves to be monitored from 2 to 80 kHz. Natural and active measurements bear complementary information about plasma regimes that are actually used in the electron density determination process.

**Acknowledgements** The authors thank all those who are in charge of CAA development, maintenance, and operations for their friendly assistance and efficiency. They also wish to express their great thanks to people from CNES who produce and deliver most of the WHISPER data products. Thanks are also due to all the scientists, research assistants, and engineers who have contributed their time to make the WHISPER experiment such a great success.

## References

1. Béghin C, Décréau PME, Pickett J, Sundkvist D, Lefebvre B (2005) Modeling of CLUSTER's electric antennas in space: application to plasma diagnostics, *Radio Science*, 40, RS6008, 1–18, doi:10.1029/2005RS003264.
2. Belmont G (1981) Characteristic frequencies of a non-Maxwellian plasma: a method for localizing the exact frequencies of magnetospheric intense natural waves near  $f_{pe}$ , *Planet. Space Sci.*, 29, 1251–1266.
3. Belmont G, Canu P, Etcheto J, de Feraudy H, Higel B, Pottelette R, Béghin C, Debrie R, Décréau PME, Hamelin M, Trotignon JG (1984) Advances in magnetospheric plasma diagnosis by active experiments, in *Proc. Conf. Achievements of the IMS*, 26–28 June 1984, Graz, Austria, ESA SP-217, 695–699.
4. Décréau PME (1983) Fonctionnement d'une sonde quadripolaire sur satellite magnétosphérique (expérience GEOS). Contribution à l'étude du comportement du plasma froid au

- voisinage de la plasmopause équatoriale, state doctorate thesis, Orléans University Orléans, France.
5. Décréau PME, Hamelin M, Massif R, De Féraudy H, Pawela E, Perraut S, Potelette R, Bahnsen A (1987) Plasma probing by active wave experiments on the Viking satellite, *Ann. Geophys. Ser. A*, 5(4), 181–186.
  6. Décréau PME, Fergeau P, Lévêque M, Martin Ph, Randriamboarison O, Sené FX, Trotignon JG, Canu P, de Féraudy H, Bahnsen A, Jespersen M, Mögensen PB, Iversen I, Dunford C, Sumner A, Woolliscroft LJC, Gustafsson G, Gurnett DA (1993) ‘WHISPER’, a Sounder and High-frequency Wave Analyser Experiment, ESA SP-1159, pp. 51–67.
  7. Décréau PME, Fergeau P, Krasnosel’skikh V, Lévêque M, Martin P, Randriamboarison O, Sené FX, Trotignon JG, Canu P, Mögensen PB, and WHISPER Investigators (1997) WHISPER, a resonance sounder and wave analyser : performances and perspectives for the CLUSTER mission, *Space Sci. Rev.*, 79, 157–193.
  8. Décréau PME, Ducoin C, Le Rouzic G, Randriamboarison O, Rauch JL, Trotignon JG, Vallières X, Canu P, Darrouzet F, Gough M, Buckley A, Carozzi T (2004) Observation of continuum radiations from the CLUSTER fleet: first results from direction finding *Ann. Geophys.* 22, 2607–2624.
  9. El-Lemdani F, Rauch JL, Décréau PME, Trotignon JG, Suraud X, Vallières X, Darrouzet F, Canu P (2009) Wave emissions at half gyroharmonics in the plasmasphere region: CLUSTER observations and statistics, *Adv. Space Res.*, 43, 253–264, doi:10.1016/j.asr.2008.06.007.
  10. Etcheto J, de Féraudy H, Trotignon JG (1981) Plasma resonance simulation in space plasmas, *Adv. Space Res.*, 1, 183–196.
  11. Etcheto J, Belmont G, Canu P, Trotignon JG (1983) Active sounder experiments on GEOS and ISEE, in: *Proc. Symp. on Active Experiments in Space*, 24–28 May 1983, Alpbach, Austria, ESA SP-195, 39–46.
  12. Gurnett DA (1998) Principles of space plasma wave instrument design, in *Measurement techniques in space plasmas: fields*, edited by Pfaff RF, Borovsky JE, Young DT, American geophysical Union, USA, pp. 121–136.
  13. Interface Control Document for WHISPER, ICD (2009) ESA, CAA-WHI-ICD-0001, issue 1.6 (<http://caa.estec.esa.int/documents/ICD/CAA.WHI.ICD.V16.pdf>).
  14. Lepine DR, Beharrel I, Bryant DA, Ely RJ, Macdougall JR, Gershuny EJ, Norris AJ (1985) Data Handling for the UKS Spacecraft, *IEEE Transactions On Geoscience And Remote Sensing*, 23, 221–229.
  15. Pedersen A, Cornilleau-Wehrlin N, De La Porte B, Roux A, Bouabdellah A, Décréau PME, Lefeuvre F, Sené FX, Gurnett D, Huff R, Gustafsson G, Holmgren G, Woolliscroft L, HStC. Alleyne, Thompson JA, Davies PNH (1997) The Wave Experiment Consortium (WEC), *Space Sci. Rev.*, 79, 157–193.
  16. Pedersen A, Lybekk B, André M, Eriksson A, Masson A, Mozer FS, Lindqvist PA, Décréau PME, Dandouras I, Sauvaud JA, Fazakerley A, Taylor M, Paschmann G, Svenes KR, Torkar K, Whipple E (2008) Electron density estimations derived from spacecraft potential measurements on CLUSTER in tenuous plasma regions, *J. Geophys. Res.*, 113, A07S33, doi:10.1029/2007JA012636.
  17. Perraut S, de Féraudy H, Roux A, Décréau PME, Paris J, Matson J (1990) Density measurements in key regions of the Earth’s magnetosphere: cusp and auroral region, *J. Geophys. Res.*, 95, 5997–6014.
  18. Perry C, Eriksson T, Escoubet P, Esson S, Laakso H, McCaffrey S, Sanderson T, Bowen H, Allen A, Harvey C (January 2006) The ESA CLUSTER Active Archive, in *Proc. CLUSTER and Double Star Symposium – 5th Anniversary of CLUSTER in Space*, 19–23 September 2005, Noordwijk, The Netherlands, ESA SP-598.
  19. Rauch JL, Suraud X, Décréau PME, Trotignon JG, Ledée R, El-Lemdani Mazouz F, Grimald S, Bozan G, Vallières X, Canu P, Darrouzet F (January 2006) Automatic determination of the plasma frequency using image processing on WHISPER data, in *Proc. CLUSTER and Double Star Symposium – 5th Anniversary of CLUSTER in Space*, 19–23 September 2005, Noordwijk, The Netherlands, ESA SP-598.

20. Serra J (1982) *Image analysis and mathematical morphology*, Vol. 1, Elsevier Academic Press London, XVIII-610 p.
21. Trotignon JG, J. Etcheto J, Thouvenin JP (1986) Automatic determination of the electron density measured by the relaxation sounder on board ISEE 1, *J. Geophys. Res.*, 91, 4302–4320.
22. Trotignon JG, Décréau PME, Rauch JL, Randriamboarison O, Krasnoselskikh V, Canu P, Alleyne H, Yearby K, Le Guirriec E, Séran HC, Sené FX, Martin Ph, Lévêque M, Ferreau P (2001) How to determine the thermal electron density and the magnetic field strength from the CLUSTER/WHISPER observations around the Earth, *Ann. Geophysicae*, 19, 1711–1720.
23. Trotignon JG, Décréau PME, Rauch JL, Le Guirriec E, Canu P, Darrouzet F (2003a) The WHISPER relaxation sounder onboard CLUSTER: a powerful tool for space plasma diagnosis around the Earth, *Cosmic Res.*, 41(4), 345–348, Translated from *Kosmicheskie Issledovaniya*, 41 369–372.
24. Trotignon JG, Rauch JL, Décréau PME, Canu P, Lemaire J (2003b) Active and passive plasma wave investigations in the earth's environment: the CLUSTER/WHISPER experiment, *Adv. Space Res.*, 31, (5)1449-(5)1454, doi: 10.1016/S0273-1177(02)00959-6
25. Trotignon JG, Décréau PME, Rauch JL, Suraud X, Grimald S, El-Lemdani Mazouz F, Vallières X, Canu P, Darrouzet F, Masson A (January 2006) The electron density around the Earth, a high level product of the CLUSTER/WHISPER relaxation sounder, in *Proc. CLUSTER and Double Star Symposium – 5th Anniversary of CLUSTER in Space*, 19–23 September 2005, Noordwijk, The Netherlands, ESA SP-598.
26. WEC Instrument User Manual, WEC UM (2000) ESA, CL-WEC-UM-002, issue 1.03 ([http://caa.estec.esa.int/caa/dwp\\_docs.xml](http://caa.estec.esa.int/caa/dwp_docs.xml)).